AM-13-053, MayJune American Mineralogist
Supplement for the article:

Incorporation of Ge in ferrihydrite: Implications for the structure of ferrihydrite

DOGAN PAKTUNC, **ALAIN MANCEAU** and **JOHN DUTRIZAC**

Unconstrained fitting of Fe-O pairs at extended *k*-range

In consideration of the absence of parameter correlations data in Maillot et al. (2011), we performed a series of simulations using the Fe-O wave function derived from goethite crystal structure (Hazemann et al., 1991; Manceau 2009) to provide a basis for evaluating the quality of the Fe-O distances and coordination numbers at the extended *k*-range of 2-17 $Å^{-1}$. The Fe-O shell is split into one sub-shell of 3O at 1.946-1.958 Å and another of 3O at 2.09-2.10 Å. Our approach is based on the Gaussian distribution approximation; therefore, the fits are considered to be physically correct without any bias.

First of all, we simulated the unfiltered theoretical Fe-O function at the extended *k*-range of 2-17 $Å^{-1}$. The simulations with the energy offset varied and fixed to 0 produced similar results (Figure S1 and Table S1). These fit parameters can be treated as nominal EXAFS values for goethite.

Table S1. Fit parameters of the theoretical Fe-O function

Fit #		*N*	*R*	σ^2	Δ*E0*	*rf*	rX^2
1	O1	3.1±0.2	1.95±0.00	0.0028	0	0.0046	853
	O2	3.1±0.2	2.09±0.00	"			
2	O1	3.0±0.1	1.95±0.00	0.0027	1.4	0.0015	337
	O2	3.0±0.1	2.10±0.00	"			

Fit performed in *R*-space (*R*=1-2.2 Å; *k*=2-17 $Å^{-1}$); amplitude reduction factor (S_0^2) is constrained to its theoretical value (here 0.8); *N*: coordination number; *R*: interatomic distance (Å); σ^2: Debye–Waller parameter ($Å^2$); Δ*E0*: energy offset (eV); *rf*: r-factor and rX^2 reduced chi-square as the goodness-of-fit parameters.

Second, we simulated the Fourier filtered Fe-O contribution from the total EXAFS spectrum at the extended *k*-range of 2-17 $Å^{-1}$ by varying and co-varying the Debye-Waller parameters of the two O shells, and by varying and fixing the energy offset to 0 (Table S2). Judging from the increased correlations among the fit parameters and the changes in the reduced chi-square values, the fit robustness deteriorated when the Debye-Waller parameters of the two O shells were floated independently (Table S2 and S3). With the exception of the energy offset, all the fitted parameters were severely correlated

(i.e. > 0.8 for Fit 3 and > 0.9 for Fit 4) when the two Debye-Waller parameters were varied independently similar to the fit strategy of Maillot et al. (2011). This finding would cast serious doubts on the accuracy of the reported precision of Maillot et al. (2011). Fixing the energy offset to decrease the degrees of freedom is not necessarily justified either as it degrades the fit quality (Table S2) without increasing the precision of the radial distances as postulated by Maillot et al. (2011).

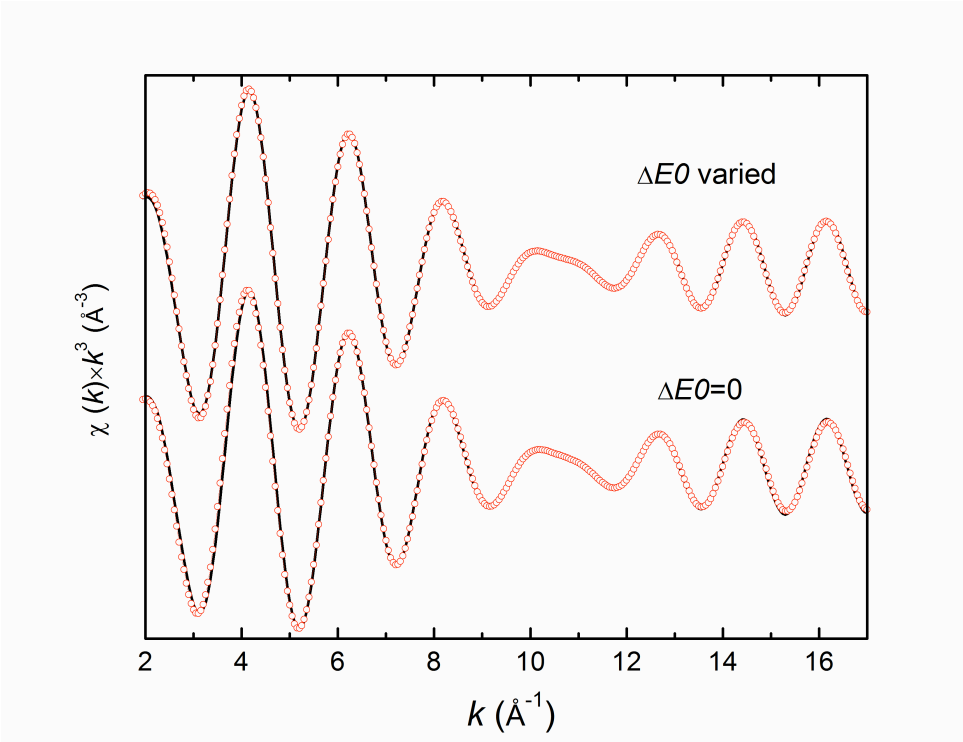

Figure S1. Theoretical Fe-O function (black) fitted with two Fe-O pairs (red circles). Top: energy offset=0; bottom: varied energy offset. Theoretical values calculated with FEFF7 are 1O at 1.946 Å, 2O at 1.958 Å, 1O at 2.09 Å and 2O at 2.10 Å, σ^2=0.0027 Å^2, Δ*E0*=0 (energy offset), and S_0^2 =0.8 (amplitude reduction factor) (Manceau, 2009). Fit parameters are given in Table S1 as fits 1 (Δ*E0*=0) and 2 (Δ*E0* floated).

Next, we performed the simulations at a shorter *k*-range (2-14 Å^{-1}), similar to Manceau (2011). In comparison to the fits performed at extended k-range (2-17 Å^{-1}) where the Debye-Waller parameters of both O shells were floated, the shorter *k*-range simulations with constrained fitting produced more robust fit. As represented by Fit 5 in Tables S2 and S3, the fit quality is better both in terms of the reduced chi-square values and parameter correlations. It appears that the correlations resulting from freeing the Debye-Waller parameters decreased the precision of the Fe-O distances to ±0.02 Å and the coordination numbers to ±0.8-0.9, which are 20% to 40% of the fit values. We conclude that there is no gain in the precision of the Fe-O distances and coordination numbers by fits performed at extended k-ranges as long as the model remains under-constrained.

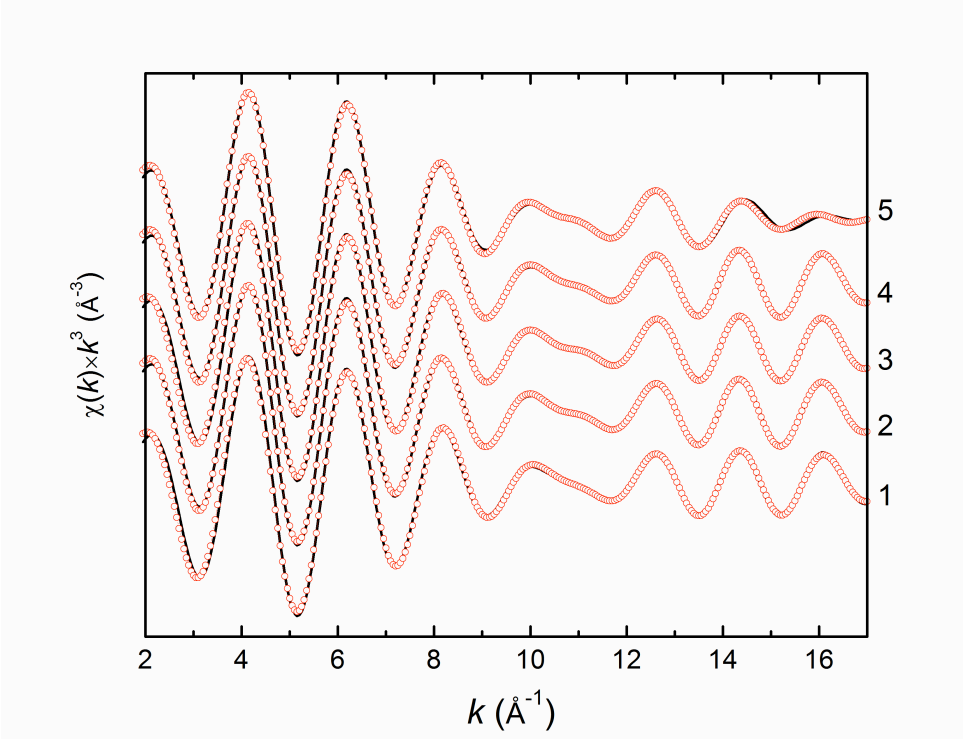

Figure S2. Fourier-transformed theoretical spectrum (black) fitted with two Fe-O pairs (red circles) at *k*-ranges of 2-17 Å^{-1} for fits 1-4 and 2-14 Å^{-1} for fit 5. Fit parameters are given in Table S2.

Table S2. Fit parameters of the Fourier filtered Fe-O function

Fit#		*N*	*R*	σ^2	Δ*E0*	*rf*	rX^2	*k*
1	O1	3.0±0.2	1.95±0.00	0.0027	0	0.0101	329	2-17
	O2	2.9±0.2	2.10±0.01	"				
2	O1	2.9±0.1	1.96±0.00	0.0025	1.7	0.0037	144	2-17
	O2	2.9±0.1	2.10±0.00	"				
3	O1	3.9±0.8	1.97±0.02	0.0041	0	0.0087	333	2-17
	O2	2.0±0.8	2.11±0.01	0.0013				
4	O1	2.5±0.9	1.95±0.02	0.0020	1.9	0.0035	171	2-17
	O2	3.3±0.9	2.10±0.02	0.0032				
5	O1	2.7±0.1	1.96±0.01	0.0020	1.6	0.0050	121	2-14
	O2	2.9±0.2	2.10±0.01	"				

Fit performed in *R*-space (*R*=1-2.2 Å; *k*=2-17 Å^{-1} or 2-14 Å^{-1}); amplitude reduction factor (S_0^2) is constrained to 0.8; *N*: coordination number; *R*: interatomic distance (Å); σ^2: Debye–Waller parameter (Å^2); Δ*E0*: energy offset (eV); *rf*: r-factor and rX^2 reduced chi-square as the goodness-of-fit parameters.

Table S3. Correlation matrices for fit parameters

Fit 1		Δ*E0*	*N O*1	*R O*1	σ^2 O1	*N O*2	*R O*2	
	Δ*E0*							
	*N O*1		1					
	*R O*1		0.21	1				
	σ^2 O1		**0.71**	0.08	1			
	*N O*2		0.61	0.20	0.60	1		
	*R O*2		0.56	0.62	0.40	0.21	1	

Fit 2		Δ*E0*	*N O*1	*R O*1	σ^2 O1	*N O*2	*R O*2	
	Δ*E0*	1						
	*N O*1	-0.35	1					
	*R O*1	0.66	-0.11	1				
	σ^2 O1	-0.14	**0.69**	-0.07	1			
	*N O*2	0.01	0.57	-0.16	0.61	1		
	*R O*2	0.59	0.20	**0.75**	0.22	0.17	1	

Fit 3		Δ*E0*	*N O*1	*R O*1	σ^2 O1	*N O*2	*R O*2	σ^2 O2
	Δ*E0*							
	*N O*1		1					
	*R O*1		**0.94**	1				
	σ^2 O1		**0.97**	**0.93**	1			
	*N O*2		**-0.89**	**-0.96**	**-0.89**	1		
	*R O*2		**0.95**	**0.97**	**0.94**	**-0.92**	1	
	σ^2 O2		**-0.82**	**-0.92**	**-0.80**	**0.96**	**-0.86**	1

Fit 4		Δ*E0*	*N O*1	*R O*1	σ^2 O1	*N O*2	*R O*2	σ^2 O2
	Δ*E0*	1						
	*N O*1	-0.66	1					
	*R O*1	-0.51	**0.97**	1				
	σ^2 O1	-0.63	**0.98**	**0.94**	1			
	*N O*2	0.62	**-0.96**	**-0.97**	**-0.92**	1		
	*R O*2	-0.49	**0.97**	**0.99**	**0.95**	**-0.95**	1	
	σ^2 O2	0.60	**-0.95**	**-0.96**	**-0.90**	**0.99**	**-0.94**	1

Fit 5		Δ*E0*	*N O*1	*R O*1	σ^2 O1	*N O*2	*R O*2	
	Δ*E0*	1						
	*N O*1	-0.21	1					
	*R O*1	**0.70**	0.15	1				
	σ^2 O1	-0.09	**0.77**	0.15	1			
	*N O*2	-0.10	0.62	-0.15	0.64	1		
	*R O*2	0.67	0.31	**0.88**	0.24	0.04	1	

Refer to Table S2 for symbols.

Detection of Ge in Fe K-edge spectra

Detection of Ge is difficult at the Fe K-edge because Fe and Ge have similar scattering amplitude and phase shift. This is illustrated by fitting the theoretical Fe-Fe function for goethite calculated with FEFF7 using 2Fe at 3.02 Å with σ^2=0.0081 Å^2 and 2Fe at 3.45 Å with σ^2=0.0081 Å^2 (Manceau, 2009). As shown in Figure S3 and Table S4 (fits 1 and 3), the inclusion of Ge instead of Fe as the second shell produced comparable fit parameters and fit qualities that are within experimental error at least above 4 Å^{-1}. In both cases, the Debye-Waller parameter of the second shell was fixed to the first shell. Although the quality of the fits improved when the Debye-Waller parameters were independently floated judging from the reduced chi-square values (Table S4), the parameter correlations were significant (Table S5) indicating that the robustness of the fits was in fact deteriorated for both instances (i.e. Fe-Fe and Fe-Ge simulations). These findings confirm the Fe-O simulations discussed previously (Table S2).

In addition, the detection of Ge is difficult at the Fe K-edge because the Fe-(Fe,Ge) shells have no sensitivity to ^{IV}Fe/^{IV}Ge, as evidenced experimentally on data from superpositioning of the imaginary parts of maghemite and six-line ferrihydrite in the 2.2 – 3.5 R+ΔR interval (Fig.8h).

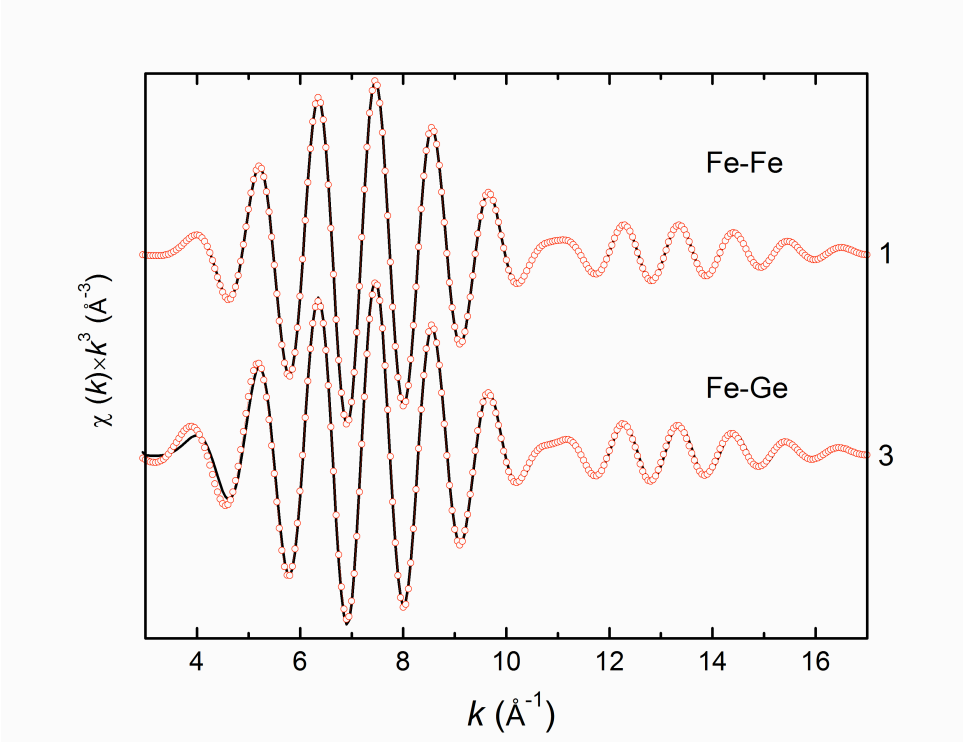

Figure S3. Theoretical Fe-Fe function (black) fitted with Fe-Fe and Fe-Fe pairs (top), and Fe-Fe and Fe-Ge pairs (bottom) (red circles). Theoretical values calculated with FEFF7 are 2Fe at 3.02 Å with σ^2=0.0081 Å and 2Fe at 3.45 Å^2 with σ^2=0.0081 Å^2. Fit parameters are given in Table S4.

Table S4. Fit parameters

Fit #		*N*	*R*	σ^2	Δ*E0*	*rf*	rX^2
1	Fe1	2.1±0.0	3.02±0.00	0.0080	0.3	0.0000	439
	Fe2	2.1±0.0	3.45±0.00	"			
2	Fe1	2.1±0.0	3.02±0.00	0.0080	0.2	0.0000	405
	Fe2	2.1±0.0	3.45±0.00	0.0081			
3	Fe	2.5±0.1	3.03±0.00	0.0087	2.8	0.0032	78977
	Ge	2.0±0.1	3.43±0.00	"			
4	Fe	1.8±0.2	3.01±0.01	0.0074	-0.1	0.0012	33412
	Ge	4.0±0.5	3.41±0.01	0.0121			

Fit performed in R-space (R=2-4 Å; *k*=3-17 $Å^{-1}$); amplitude reduction factor (S_0^2) is constrained to 1; *N*: coordination number; *R*: interatomic distance (Å); σ^2: Debye–Waller parameter ($Å^2$); Δ*E0*: energy offset (eV); *rf*: r-factor and rX^2 reduced chi square as the goodness-of-fit parameters; For fits 1 and 2, the Debye-Waller parameters of subsequent shells were constrained to be identical with the initial shell values.

Significance of the differences in the measured Fe-O EXAFS distances in ferrihydrite

Using the Fe-O interatomic distances and coordination numbers determined by shell-by-shell fitting of the Fe EXAFS data, we re-calculated the proportion of tetrahedral iron in the five ferrihydrite samples studied by Maillot et al. (Fig. S4). Our results are different from those reported by Maillot et al. (2011). A close examination of their paper revealed further discrepancies. The numbers for ferrihydrite reported in the text and tables do not match those presented in their Figure 2. We determined the uncertainties in the average Fe-O distances and the tetrahedral iron by two different approaches. First, we determined the variations of the coordination numbers from the quoted error values of 20% on each oxygen shell and 10% on the sum, and carried over the uncertainties on individual shells to calculating the uncertainty on the average Fe-O distances and the tetrahedral iron. The results indicate that the uncertainties of the average Fe-O distances are ±0.016-0.022 Å and those in the proportion of tetrahedral Fe are ±0.10-0.15 (Fig. S4a, red symbols and lines). Our second approach involved taking into consideration of all combinations of minimum and maximum Fe-O distances (i.e. ±0.01 Å) and minimum and maximum coordination numbers (i.e. 10% on the average of the sum of the coordination numbers reported by Maillot et al. 2011). The uncertainties are ±0.012-0.015 Å for the Fe-O distances and ±0.09-0.10 for the proportion of tetrahedral iron (Fig. S4a, blue symbols and error bars). Both approaches indicate that uncertainties are much greater than those depicted by Maillot et al. (2011). The tetrahedral iron formula of Maillot et al. (2011) implies the presence of 12% tetrahedral iron in their akaganeite sample, which is another indication of the limitation of the approach.

As demonstrated earlier, more realistic uncertainties in the EXAFS determination of coordination numbers would be 30% for each shell (Table S2) for a fitting strategy adopted by Maillot et al. (2011). The use of this uncertainty value for each shell and

±0.01 Å for the Fe-O distances in all possible combinations would increase the standard deviations of the average Fe-O distances to ±0.022-0.028 Å and those of the tetrahedral iron to ±0.24 (Fig. S4b).

These calculations indicate that the differences in the Fe-O distances between the ferrihydrites and akaganeite, and to a lesser extent goethite, reported by Maillot et al. (2011) are statistically insignificant.

Table S5. Correlation matrices for fit parameters

Fit1		Δ*E0*	*N* Fe1	*R* Fe1	σ^2 Fe1	*N* Fe2	*R* Fe2
	Δ*E0*	1					
	N Fe1	0.26	1				
	R Fe1	**0.93**	0.39	1			
	σ^2 Fe1	0.09	**0.88**	0.23	1		
	N Fe2	-0.28	0.47	-0.20	**0.71**	1	
	R Fe2	**0.92**	0.26	**0.83**	0.05	-0.28	1

Fit2		Δ*E0*	*N* Fe1	*R* Fe1	σ^2 Fe1	*N* Fe2	*R* Fe2	σ^2 Fe2
	Δ*E0*	1						
	N Fe1	**0.79**	1					
	R Fe1	**0.97**	**0.82**	1				
	σ^2 Fe1	0.66	**0.95**	**0.71**	1			
	N Fe2	**-0.82**	**-0.75**	**-0.80**	-0.58	1		
	R Fe2	**0.97**	**0.75**	**0.93**	0.61	**-0.78**	1	
	σ^2 Fe2	**-0.71**	-0.60	-0.67	-0.42	**0.95**	-0.68	1

Fit3		Δ*E0*	*N* Fe	*R* Fe	σ^2 Fe	*N Ge*	*R Ge*
	Δ*E0*	1					
	N Fe	0.15	1				
	R Fe	**0.93**	0.27	1			
	σ^2 Fe	0.05	**0.88**	0.17	1		
	N Ge	-0.24	0.53	-0.21	**0.72**	1	
	R Ge	**0.89**	0.18	**0.82**	0.02	-0.24	1

Fit4		Δ*E0*	*N* Fe	*R* Fe	σ^2 Fe	*N Ge*	*R Ge*	σ^2 Ge
	Δ*E0*	1						
	N Fe	**0.81**	1					
	R Fe	**0.97**	**0.84**	1				
	σ^2 Fe	0.65	**0.93**	**0.71**	1			
	N Ge	**-0.83**	**-0.79**	**-0.81**	-0.59	1		
	R Ge	**0.98**	**0.79**	**0.95**	0.62	**-0.81**	1	
	σ^2 Ge	**-0.74**	-0.68	**-0.70**	-0.45	**0.97**	**-0.73**	1

Refer to Table S4 for symbols.

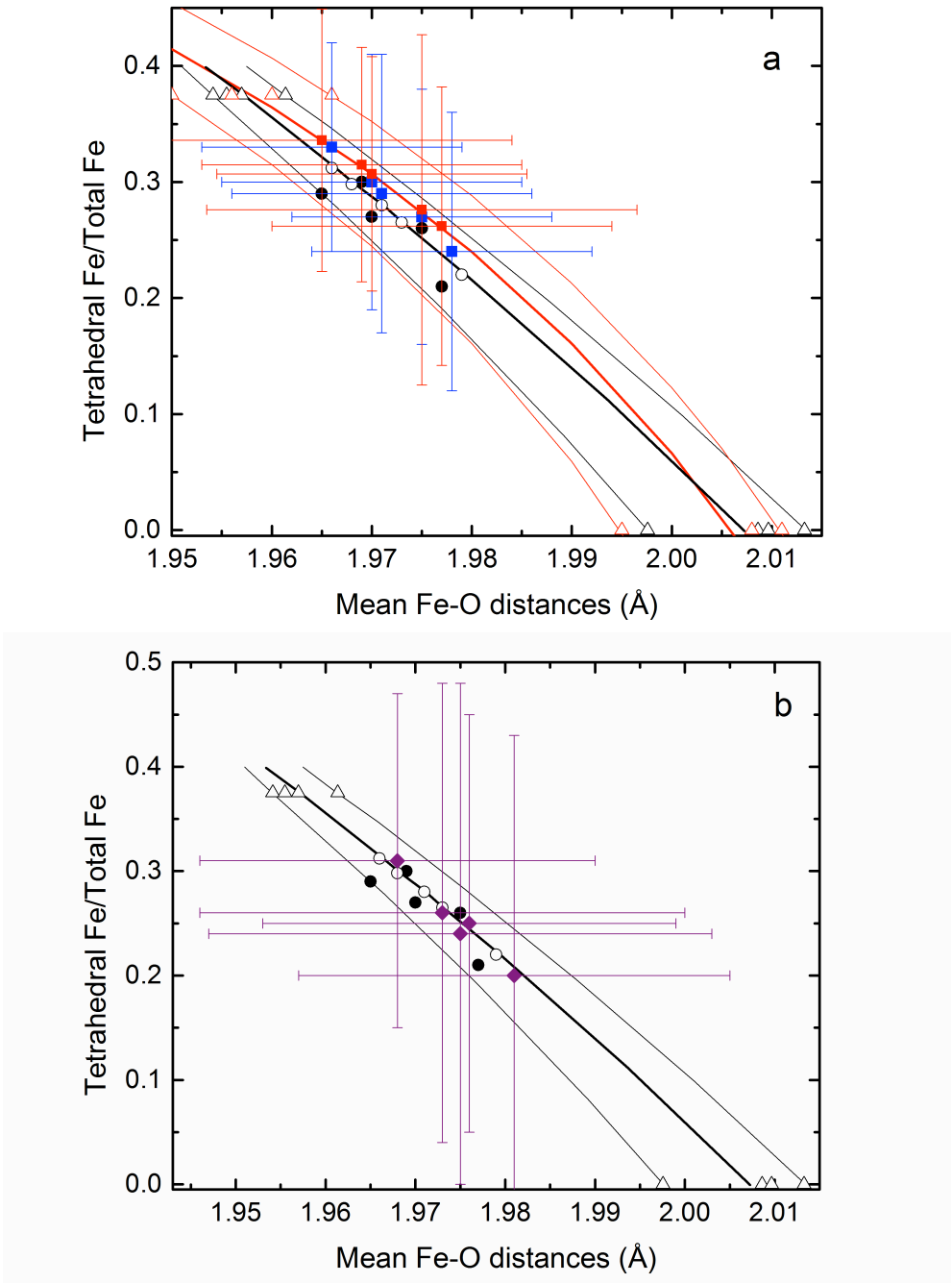

Figure S4. Variation of tetrahedral iron with mean Fe-O distances calculated from data on Table EA-1 of Maillot et al. (2011). Black regression lines and open symbols were reproduced from Fig.2a of Maillot et al. (2011). Solid black symbols are based on mean Fe-O distances calculated from data on Table EA-1 and tetrahedral iron values reported on page 2715 of Maillot et al. (2011). (a) Red symbols and lines representing regression lines were calculated from raw data on Table EA-1 with 1.958 Å Fe-O value for tetrahedral iron and 2.006 Å for octahedral iron; Blue symbols and error bars were derived from averaging two Fe-O distances by weighting with coordination numbers and taking into consideration of the associated uncertainties (i.e. ±0.01 Å on both Fe-O distances and10% on the sum of O1 and O2 coordination numbers); (b) Purple symbols and error bars were calculated by assuming

uncertainty values of ±0.01 Å on both Fe-O distances and 30% on coordination numbers.

REFERENCES CITED

Hazemann, J.L., Berar, J.F., and Manceau, A. (1991) Rietveld studies of the aluminium-iron substitution in synthetic goethite. Materials Sciences Forum, 79-82, 821-826.

Maillot, F., Morin, G., Wang, Y., Bonnin, D., Ildefonse, P., Chaneac, C., and Calas, G. (2011). New insight into the structure of nanocrystalline ferrihydrite: EXAFS evidence for tetrahedrally coordinated iron(III). Geochimica et Cosmochimica Acta, 75, 2708-2720.

Manceau, A (2009) Evaluation of the structural model for ferrihydrite derived from real-space modeling of high-energy X-ray diffraction data. Clay Minerals, 44, 19-34.

_____ (2011) Critical evaluation of the revised akdalaite model for ferrihydrite. American Mineralogist, 96, 521–533.